Monthly Notices
of the
ROYAL ASTRONOMICAL SOCIETY

MNRAS **438,** 841–845 (2014)
Advance Access publication 2013 December 13

doi:10.1093/mnras/stt2249

Experimental Stark widths and shifts of Cr II spectral lines

J. A. Aguilera,[1]★ C. Aragón[1]★ and J. Manrique[2]

[1]*Departamento de Física, Universidad Pública de Navarra, Campus de Arrosadía, E-31006 Pamplona, Spain*
[2]*Facultad de Farmacia, Universidad CEU San Pablo, Urbanización Montepríncipe, Boadilla del Monte, E-28668 Madrid, Spain*

Accepted 2013 November 18. Received 2013 November 15; in original form 2013 November 4

ABSTRACT

Stark widths and shifts of Cr II lines with wavelengths in the range 2000–3500 Å have been determined by laser-induced breakdown spectroscopy. The spectra have been measured at different instants of the plasma evolution from 0.6 to 3.4 μs, at which the temperature and electron density are in the ranges 12 000–16 300 K and (0.89–8.2) × 10^{17} cm^{-3}, respectively. The laser-induced plasmas have been generated from three fused glass samples with different chromium concentrations, selected to control the self-absorption of the lines. The Stark widths and shifts are compared with the experimental and theoretical data available in the literature.

Key words: atomic data – line: profiles – plasmas.

1 INTRODUCTION

The knowledge of Stark broadening and shift parameters is of interest for atomic structure studies, as well as for diagnostics of laboratory and astrophysical plasmas. In the particular case of chromium, a large number of lines of the ionized atom are identified in the spectra of chemically peculiar stars. For example, Cr II lines can be found in the spectra of A-type stars as 7 Sex (Adelman & Philip 1996) and φ Aqu (Caliskan & Adelman 1997), where Stark broadening is the most significant pressure broadening mechanism.

Despite their relevance, experimental and theoretical data for Cr II Stark widths and shifts are scarce. Rathore et al. (1984) performed the only experimental determination of the Stark widths and shifts for Cr II spectral lines using a T-tube plasma, including the parameters of three lines from the multiplet 4s ^{4}D–4p ^{4}F^o. Lakićević (1983) estimated the Stark width and shift of the Cr II line at 2065.65 Å on the basis of regularities and systematic trends. Dimitrijević et al. (2007) calculated Stark widths and shifts within the semiclassical perturbation approach for the lines of seven Cr II multiplets from the 4s–4p transitions and Simić, Dimitrijević & Sahal-Bréchot (2013) have recently reported calculations of these parameters for nine Cr II resonant $3d^5$–$3d^4$4p multiplets using the same approach. The data obtained by Dimitrijević et al. (2007) could be compared with the experimental results of Rathore et al. (1984) and an acceptable agreement is reported by the authors, although is noted the accuracy of 50 per cent attributed by Konjević & Wiese (1990) to these experimental results. The latter theoretical works have applied the Stark parameters to the analysis of Cr II line profiles in astrophysical plasmas and the authors concluded its importance for stellar atmosphere modelling and the need of new Stark parameters for the Cr II lines. Other astrophysical applications of the Stark parameters of the Cr II lines are reported in the review by Sahal-Bréchot (2010), referring to the need of new data due to the development of space-borne spectroscopy.

In previous works, our group has used laser-induced breakdown spectroscopy (LIBS) for the measurement of Stark widths, as examples see Aguilera, Aragón & Manrique (2013) and Aragón, Aguilera & Manrique (2013). In the latter work, the use of fused glass samples is shown to be advantageous for Stark width measurements by LIBS. In this work, we make use of this method to provide new values of Stark widths and shifts for Cr II lines, reporting data for wavelengths in the range 2000–3500 Å.

2 EXPERIMENT

The experimental setup is similar to that used previously (Aguilera et al. 2013), so only a brief description with the emphasis in new features is given here. The laser-induced plasmas are generated using a Nd:YAG laser (wavelength 1064 nm, pulse energy 60 mJ, pulse width 4.5 ns, repetition rate 20 Hz) focused on to the sample surface in air at atmospheric pressure. The focusing lens has 128 mm focal length and the lens-to-sample distance is 124 mm. The light emitted from the plasma is collected in a direction forming a small angle with the laser beam by a system of flat and concave mirrors forming a 1:1 image of the plasma on the entrance slit of a 0.75 m Czerny–Turner spectrometer equipped with a time-resolved intensified CCD (1200 × 256 effective pixels). The grating (3600 and 1200 lines mm^{-1}) and the slit width (20 and 50 μm) are selected according to the spectral resolution needed.

Three fused glass samples have been prepared from pure chromium oxide with chromium atomic concentrations of 0.05, 0.1 and 0.2 per cent. During the measurements, the emission

★ E-mail: j.a.aguilera@unavarra.es (JAA); carlos.aragon@unavarra.es (CA)

of 100 laser shots is accumulated while the sample rotates at 100 rev min^{-1}.

3 RESULTS AND DISCUSSION

The spectra of the plasma emission have been obtained with six time windows having different delays from the laser pulse, centred at instants of the plasma lifetime ranging from 0.6 to 3.4 μs. The width of the time windows increases with the delay from 0.06 to 0.6 μs. The characterization of the plasma generated from the fused glass samples has been carried out as in the previous work (Aragón et al. 2013). The temperature has been determined by means of a Boltzmann plot constructed from seven Fe II lines, using samples prepared with a small iron content of 0.8 per cent, the percentage being expressed in atom number densities. The temperature decreases from 16 300 ± 200 K at 0.6 μs to 12 000 ± 150 K at 3.4 μs, where the error has been estimated as the standard deviation of the slope of the linear fitting of the Boltzmann plot.

The determination of the electron density is based on the Stark broadening of the Hα line, whose emission arises from the small water content of air surrounding the sample. In spite of the known inhomogeneity of laser-induced plasmas, it was shown in a previous work (Aragón & Aguilera 2010) that, in spatially integrated measurements, the electron density values obtained from lines of singly ionized atoms and from the Hα line agree within 3 per cent. The Hα spectra were obtained using the grating of 1200 lines mm^{-1} and a spectrometer slit of 50 μm. This configuration leads to an instrumental width of 55 pm, much lower than the Lorentzian width of the Hα line. The latter has been determined by fitting the spectra to Voigt profiles with a Gaussian width given by the combination of the instrumental width and the Doppler width. To obtain the electron density from the line width of the Hα line, the diagnosis tables of Gigosos & Cardeñoso (1996) have been used. The electron density decreases from 8.2×10^{17} cm^{-3} at 0.6 μs to 0.89×10^{17} cm^{-3} at 3.4 μs. The error of these measurements is estimated to be 11 per cent, caused by the propagation of the error of the Stark width of Hα reported in the diagnosis tables, whereas the statistical error is negligible in comparison.

As shown in the previous work (Aragón et al. 2013), the self-absorption of the spectral lines in laser-induced plasmas generated from fused glass samples has a limited effect due to the low concentration in the sample that leads to a suitable signal-to-background ratio. The Cr concentration in the sample has been selected for the Cr II lines with the help of the k_t coefficient, defined as (Aragón, Peñalba & Aguilera 2005)

$$k_t = \frac{e^2\lambda_0^2}{4\varepsilon_0 mc^2} f \frac{g_i e^{-\frac{E_i}{kT}}}{U(T)} \left(1 - e^{-\frac{E_k - E_i}{kT}}\right), \quad (1)$$

where e is the elementary charge, λ_0 is the central wavelength of the emission line, ε_0 is the permittivity of free space, m is the electron mass, c is the speed of light in vacuum, f is the transition oscillator strength, g_i is the degeneracy of the lower energy level, E_i and E_k are the energies of the lower and upper energy levels, respectively, k is the Boltzmann's constant, T is the temperature and $U(T)$ is the partition function. To calculate the k_t coefficient, the level energies, degeneracies and oscillator strengths of the Cr II lines are taken from Nilsson et al. (2006), Kramida et al. (2013) and Kurucz & Bell (1995). The more intense lines at 2835.629, 2843.249 and 2766.531 Å have k_t values, calculated at a temperature of 14 000 K and expressed in units of 10^{-30} m^3, of 18.1, 11.7 and 9.75, respectively. For these lines, a concentration of 0.05 atomic per cent has been used, as done in Aragón et al. (2013) for Ni II lines with k_t values of the same order of magnitude. For lines of moderate intensity, with k_t values in the range (4.40–7.74) × 10^{-30} m^3, the sample with a Cr content of 0.1 atomic per cent is used. The rest of the lines are weaker, having lower k_t values; these lines are measured using the sample with a 0.2 per cent concentration. It is worth noting that for the lines of the multiplet a^6D–z^6F^o, having very different k_t values, the final measured values of the Stark width were the same within the experimental error, a fact that supports the small effect of self-absorption in the measurements.

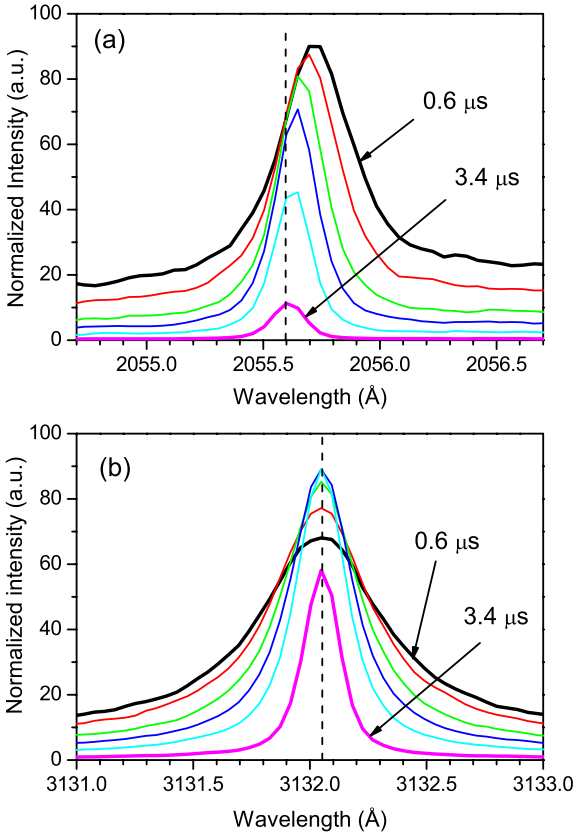

Figure 1. Spectra of Cr II lines at 2055.596 Å (a) and 3132.053 Å (b) obtained at different time windows from 0.6 to 3.4 μs.

To measure the Stark widths and shifts of the Cr II lines, the spectra have been obtained with the grating of 3600 lines mm^{-1} and a slit width of 20 μm, so that the instrumental width is reduced to 13.5 pm. The spectra of two Cr II lines obtained at the different time windows are shown in Fig. 1. In these plots, the intensity is normalized to the width of the time window used in each case. The decrease of the line width for increasing delay from the laser pulse, due to the temporal decay of the electron density, can be observed for both lines. However, we see in Fig. 1(a) that the line at 2055.596 Å shows clearly a redshift that decreases for increasing delay, whereas for the line at 3132.053 Å, as shown in Fig. 1(b), the shift is hardly noticeable. To determine the line widths and shifts, the spectra have been fitted to Voigt profiles using a home-made least-squares computer program. The Gaussian width is given by the combination of the instrumental width and the Doppler width, the latter estimated as 3 pm for a typical temperature of 14 000 K. One of such fittings, for the line at 2055.596 Å at the time window

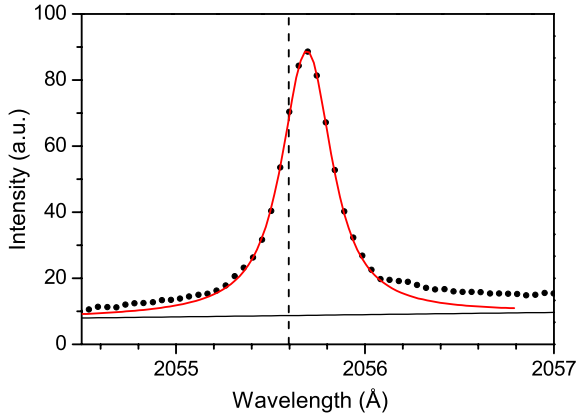

Figure 2. Spectrum of the Cr II line at 2055.596 Å and fitting to a Voigt profile. The dashed line shows the position of the unshifted line.

centred at 0.74 μs, is shown in Fig. 2, where the dashed line indicates the wavelength taken as reference for shift measurements. This wavelength is obtained from the spectrum at 10 μs delay, when the Stark shift is negligible. The Lorentzian width obtained for this line at the different time windows is in the range 3.1–30 pm, while the shift varies from 0.55 to 12 pm. It should be noted that the error of the Stark shift values is small due to the fact that the fitting is carried out for a large number of points, as shown in Fig. 2, so that the central wavelength of the Voigt profile is provided accurately. Therefore, small shifts have been reported, although, because of the resolution of the measurement of the central wavelength, an absolute error higher than 0.1 pm has been considered.

The line widths measured for two Cr II lines are shown in Fig. 3(a) as a function of the electron density, while Fig. 3(b) shows the line shifts. As can be seen in both plots, we have found proportionality between the determined line widths and shifts and the corresponding electron density at each instant. Taking into account the experimental error, the weak dependence of Stark width and shift on temperature has not been observed. Therefore, the final results are obtained as the slopes of the linear fittings of these plots with zero intercept, this value corresponds to the Stark width (FWHM) and shift at an electron density of 10^{17} cm^{-3}. The results obtained for the Stark widths and shifts range from 3.4 to 12 pm and −0.4 to 1.6 pm, respectively, and are presented in Table 1 arranged by transition and multiplet, together with previous results from the literature. Table 2, available online as Supporting Information, presents our results sorted by air wavelength and compared to previous results. The Stark widths are determined as full width at half-maximum (FWHM) values. The experimental relative error of Stark widths has been estimated as 15 per cent by adding quadratically the error of the electron density (11 per cent), the error caused by self-absorption (10 per cent) and the uncertainty due to plasma inhomogeneity (3 per cent). In the case of the Stark shifts, as mentioned before, the minimum absolute error due to resolution is 0.1 pm. However, for shifts clearly exceeding this value, a relative error of 11 per cent is estimated from the electron density uncertainty and the plasma inhomogeneity, assuming that self-absorption does not involve a shift of lines.

For the three lines with previous experimental values (Rathore et al. 1984), measured using a T-tube neon plasma, the widths are higher than ours by a factor of 3 whereas the shifts are much

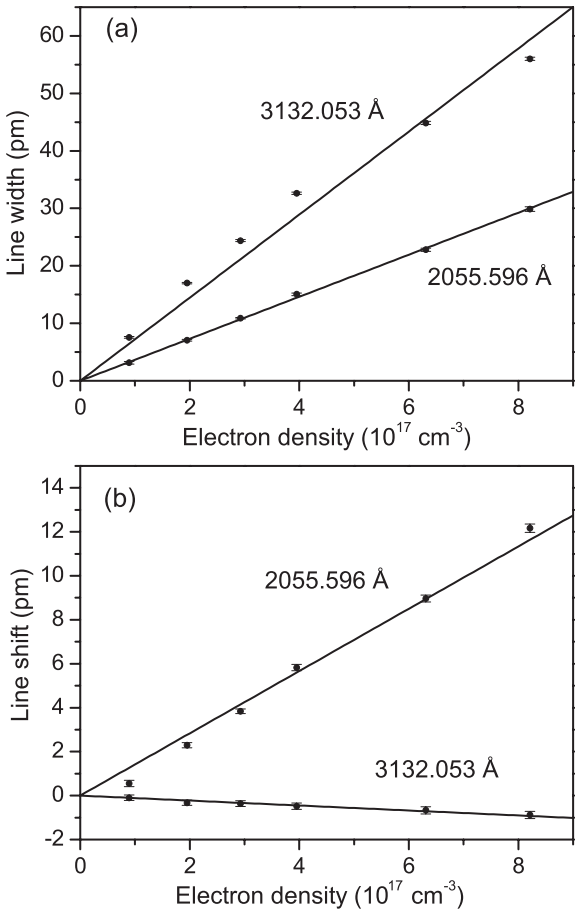

Figure 3. Line width (a) and shift (b) of Cr II lines at 2055.596 Å and 3132.053 Å as a function of the electron density.

larger. Theoretical calculations based on the semiclassical perturbation approach reported by Dimitrijević et al. (2007) show the same behaviour in relation to our results, the widths being higher than our data by 2–3 factors. On the other hand, the calculated widths reported by Simić et al. (2013) for resonant $3d^5$–$3d^4$4p multiplets are in good agreement with our experimental data, while the shifts calculated in this reference for the a^6S–z^6P^o multiplet have opposite sign and smaller values than ours.

4 CONCLUSIONS

We report measurements of Stark widths and shifts of Cr II lines with wavelengths in the range 2000–3500 Å carried out by LIBS. The use of fused glass samples and the method employed to control the self-absorption of the lines, based on the selection of the chromium concentration in the sample, has allowed us to provide data for 45 multiplets, including 83 widths and 49 shifts, all of them first measured with the exception of three lines.

ACKNOWLEDGEMENTS

This work has been supported by the project FIS2011-29521 of the Spanish Ministerio de Economía y Competitividad.

Table 1. Stark widths (FWHM) w (pm) and shifts d (pm) at electron density 10^{17} cm^{-3} of Cr II spectral lines, compared to experimental and theoretical values reported in the literature. The temperature range is 12 000–16 300 K. The relative error of w is 15 per cent. The relative error of d is 11 per cent, with a minimum absolute error of 0.1 pm.

				Experimental					Theoretical		
No.	Transition	Multiplet	λ (Å)	w	d	w^a	d^a	w^b	w^c	d^b	d^c
1	$3d^5$–$3d^4(^5D)4p$	$a\,^6S$–$z\,^6P^\star$	2055.596	3.7	1.4				3.42		−0.0402
			2061.575	3.4	1.4				3.42		−0.0402
2	$3d^4(^5D)4s$–$3d^4(^5D)4p$	$a\,^6D$–$z\,^6F^\star$	2835.629	5.0	0.1						
			2843.249	5.1	0.0						
			2849.837	5.1	− 0.1						
			2855.670	5.0							
			2860.934	5.0	− 0.2						
			2862.571	4.7							
3		$a\,^6D$–$z\,^6P^\star$	2766.531	4.4	− 0.1			10.0		− 0.927	
			2762.589	4.5				10.0		− 0.927	
			2757.720	4.7	− 0.1			10.0		− 0.927	
			2751.864	4.8	− 0.1			10.0		− 0.927	
			2750.727	5.1	− 0.1			10.0		− 0.927	
			2748.980	5.0				10.0		− 0.927	
			2743.641	5.1				10.0		− 0.927	
4		$a\,^6D$–$z\,^4P^\star$	2672.826	5.4	− 0.2						
			2712.303	5.9	− 0.2						
			2653.578	5.3	− 0.1						
5		$a\,^6D$–$z\,^6D^\star$	2691.040	4.3	0.3			10.2		− 0.0738	
			2671.803	4.6	0.2			10.2		− 0.0738	
			2668.707	4.6	0.1			10.2		− 0.0738	
			2666.020	4.8	0.3			10.2		− 0.0738	
			2678.789	5.0				10.2		− 0.0738	
6		$a\,^6D$–$z\,^4F^\star$	2534.333	5.3							
7		$a\,^4D$–$z\,^4P^\star$	3368.041	9.1	− 0.2			29.7		− 9.52	
			3422.732	8.5				29.7		− 9.52	
			3342.576	8.7	− 0.2			29.7		− 9.52	
			3421.202	8.9				29.7		− 9.52	
8		$a\,^4D$–$z\,^4F^\star$	3132.053	7.2	− 0.1	34	−10	27.8		− 9.06	
			3124.973	7.4	− 0.1	26	−12	27.8		− 9.06	
			3120.359	7.5	− 0.2	22.6	−11	27.8		− 9.06	
			3118.646	7.6	− 0.2			27.8		− 9.06	
			3147.220	7.5	− 0.2			27.8		− 9.06	
			3128.692	7.1	− 0.2			27.8		− 9.06	
9		$a\,^4D$–$z\,^4D^\star$	2870.432	6.5	0.4			22.3		− 7.06	
			2880.863	6.9	0.3			22.3		− 7.06	
10	$3d^4(^5D)4s$–$3d^4(^3F)4p$	$a\,^4D$–$y\,^4F^\star$	2107.944	4.1							
11	$3d^5$–$3d^4(^5D)4p$	$a\,^4G$–$z\,^4F^\star$	3180.693	10.7					10.8		1.97
			3209.176	10.9					10.8		1.97
12	$3d^5$–$3d^4(^3H)4p$	$a\,^4G$–$z\,^4H^\star$	2297.169	4.7	1.6						
			2314.721	5.0	1.5						
13	$3d^5$–$3d^4(^5D)4p$	$b\,^4D$–$z\,^4D^\star$	3360.291	12.1					10.8		0.392
14	$3d^5$–$3d^4(a\,^3P)4p$	$b\,^4D$–$y\,^4P^\star$	2397.748	5.9	1.6						
15	$3d^4(^3P)4s$–$3d^4(a\,^3P)4p$	$b\,^4P$–$y\,^4D^\star$	2935.132	6.6							
			2930.847	6.6	− 0.1						
			2976.709	6.0	− 0.1						
			2961.721	6.2	− 0.2						
16	$3d^5$–$3d^4(^1I)4p$	$a\,^2I$–$w\,^2H^\star$	2121.257	4.7							
17	$3d^4(^3H)4s$–$3d^4(^3H)4p$	$a\,^4H$–$z\,^4H^\star$	2971.899	7.1							
			2979.736	7.0	− 0.4						
			2989.190	6.8							
18		$a\,^4H$–$z\,^4I^\star$	2840.013	5.4	0.1						
			2851.354	5.6							
19		$a\,^4H$–$y\,^4G^\star$	2693.528	4.9	0.2						
20	$3d^4(^3H)4s$–$3d^4(^3G)4p$	$a\,^4H$–$y\,^4H^\star$	2584.107	4.0							
21	$3d^4(^3F)4s$–$3d^4(a\,^3P)4p$	$a\,^4F$–$y\,^4D^\star$	2966.038	5.5	0.2						
			3003.911	6.2							
22	$3d^4(^3F)4s$–$3d^4(a^3F)4p$	$a\,^4F$–$z\,^4G^\star$	2936.933	7.2	0.0						
23		$a\,^4F$–$x\,^4D^\star$	2727.254	5.5							
24	$3d^4(^3G)4s$–$3d^4(^3H)4p$	$b\,^4G$–$z\,^4H^\star$	3295.423	7.9	− 0.4						

Table 1 – *continued*

				Experimental		Theoretical					
No.	Transition	Multiplet	λ (Å)	w	d	w^a	d^a	w^b	w^c	d^b	d^c
25	$3d^4(^3G)4s–3d^4(a\ ^3F)4p$	$b\ ^4G–z\ ^4G^\star$	3122.596	6.3	0.1						
26	$3d^4(^3G)4s–3d^4(^3G)4p$	$b\ ^4G–y\ ^4H^\star$	2800.758	6.4							
27		$b\ ^4G–^4F^\star$	2792.151	5.4	0.0						
			2785.692	5.7							
28	$3d^4(^3H)4s–3d^4(^3H)4p$	$a\ ^2H–z\ ^2I^\star$	3050.130	7.5	1.0						
			3040.924	8.0							
29	$3d^4(^3H)4s–3d^4(a\ ^3F)4p$	$a\ ^2H–y\ ^2G^\star$	2832.452	6.2	0.9						
30	$3d^4(^3P)4s–3d^4(a\ ^3P)4p$	$a\ ^2P–z\ ^2S^\star$	3291.763	9.2							
31		$a\ ^2P–z\ ^2P^\star$	3172.070	7.8	−0.1						
32	$3d^4(^3P)4s–3d^4(a\ ^3F)4p$	$a\ ^2P–y\ ^4F^\star$	3152.213	7.2	−0.2						
33	$3d^4(^3F)4s–3d^4(a\ ^3F)4p$	$b\ ^2F–y\ ^4F^\star$	3183.326	8.5							
34		$b\ ^2F–z\ ^2F^\star$	3028.124	7.7							
35	$3d^5–3d^4(^3H)4p$	$b\ ^2H–z\ ^2H^\star$	3041.720	9.2							
36	$3d^5–3d^4(^1I)4p$	$b\ ^2H–^2I^\star$	2575.788	5.7							
37	$3d^5–3d^4(a\ ^1G)4p$	$b\ ^2H–x\ ^2H^\star$	2573.532	7.8							
38	$3d^5–3d^4(^1I)4p$	$b\ ^2H–w\ ^2H^\star$	2416.393	6.2							
39	$3d^5–3d^4(a\ ^1D)4p$	$a\ ^2G–v\ ^2F^\star$	2215.065	5.3							
40	$3d^4(^3D)4s–3d^4(^3D)4p$	$c\ ^4D–w\ ^4D^\star$	2838.778	5.5	0.2						
41	$3d^4(^3G)4s–3d^4(^3G)4p$	$b\ ^2G–x\ ^4G^\star$	3107.563	7.9							
42		$b\ ^2G–x\ ^2G^\star$	2927.083	6.9							
43	$3d^4(a\ ^1G)4s–3d^4(a\ ^1G)4p$	$c\ ^2G–w\ ^2G^\star$	2774.430	6.3	1.3						
44	$3d^5–3d^4(a\ ^3F)4p$	$c\ ^2F–y\ ^2G^\star$	3306.955	7.8	0.0						
45	$3d^4(^3D)4s–3d^4(^3D)4p$	$b\ ^2D–w\ ^2F^\star$	2941.957	6.6	0.7						

[a]Rathore et al. (1984). Temperature 13 700 K.
[b]Dimitrijević et al. (2007). Data interpolated to a temperature of 14 000 K.
[c]Simić et al. (2013). Data interpolated to a temperature of 14 000 K.

REFERENCES

Adelman J., Philip A. G., 1996, MNRAS, 282, 1181
Aguilera J. A., Aragón C., Manrique J., 2013, J. Quant. Spectrosc. Radiat. Transfer, 114, 151
Aragón C., Aguilera J. A., 2010, Spectrochim. Acta B, 65, 395
Aragón C., Peñalba F., Aguilera J. A., 2005, Spectrochim. Acta B, 60, 879
Aragón C., Aguilera J. A., Manrique J., 2013, J. Quant. Spectrosc. Radiat. Transfer, in press, doi:10.1016/j.jqsrt.2013.10.011
Caliskan H., Adelman J., 1997, MNRAS, 288, 501
Dimitrijević M. S., Ryabchikova T., Simić Z., Popović L. Č., Dačić M., 2007, A&A, 469, 681
Gigosos M. A., Cardeñoso V., 1996, J. Phys. B: At. Mol. Opt. Phys., 29, 4795
Konjević N., Wiese W. L., 1990, J. Phys. Chem. Ref. Data, 19, 1307
Kramida A., Ralchenko Yu., Reader J., NIST ASD Team, 2013, NIST Atomic Spectra Database (version 5.1), available at: http://physics.nist.gov/asd
Kurucz R. L., Bell B., 1995, Atomic Line Data CD-ROM No. 23. Smithsonian Astrophysical Observatory, Cambridge
Lakićević I. S., 1983, A&A, 127, 37
Nilsson H., Ljung G., Lundberg H., Nielsen K. E., 2006, A&A, 445, 1165
Rathore B. A., Lakićević I. S., Ćuk M., Purić J., 1984, Phys. Lett. A, 100, 31
Sahal-Bréchot S., 2010, J. Phys.: Conf. Ser., 257, 012028
Simić Z., Dimitrijević M. S., Sahal-Bréchot S., 2013, MNRAS, 432, 2247

SUPPORTING INFORMATION

Additional Supporting Information may be found in the online version of this article:

Table 2. Stark widths (FWHM) w (pm) and shifts d (pm) at electron density 10^{17} cm^{-3} of Cr II spectral lines, compared to experimental and theoretical values reported in the literature. Transitions sorted by wavelength. The temperature range is 12 000–16 300 K (http://mnras.oxfordjournals.org/lookup/suppl/doi:10.1093/mnras/stt2249/-/DC1).

Please note: Oxford University Press are not responsible for the content or functionality of any supporting materials supplied by the authors. Any queries (other than missing material) should be directed to the corresponding author for the article.

This paper has been typeset from a Microsoft Word file prepared by the author.